

Characterization of light scattering in translucent ceramics

M. A. Illarramendi and I. Aramburu

*Departamento de Física Aplicada I, Escuela Técnica Superior de Ingeniería, Universidad del País Vasco,
Alda. Urquijo s/n, 48013 Bilbao, Spain*

J. Fernandez and R. Balda

*Departamento de Física Aplicada I, Escuela Técnica Superior de Ingeniería, Universidad del País Vasco,
Alda. Urquijo s/n, 48013 Bilbao, Spain, and Unidad Física de Materiales CSIC-UPV/EHU and Donostia International
Physics Center Apartado 1072, 20080 Donostia, Basque Country, Spain*

S. N. Williams, J. A. Adegoke, and M. A. Noginov

Center for Materials Research, Norfolk State University, Norfolk, Virginia 23504, USA

Received July 28, 2006; accepted September 13, 2006;
posted September 29, 2006 (Doc. ID 73537); published December 20, 2006

We have obtained expressions for the reflectance and transmittance of a scattering medium with weak absorption in terms of a diffusion model, where the source is an incoming beam, whose intensity exponentially decays along the propagation path. We have applied three experimental techniques, one of which is based on the developed model, to determine the transport mean-free-path in translucent samples of Nd:YAG ceramics.

© 2006 Optical Society of America

OCIS codes: 160.3380, 160.5690, 290.0290.

1. INTRODUCTION

Scattering is one of the important characteristics of optical materials. Often the applications of optical materials require scattering to be low. This is the case for optical windows, fibers, active elements of regular lasers, etc. At the same time, other applications (including diffusive reflectors, random lasers, etc.) benefit from high scattering.

The two most important parameters characterizing scattering are the scattering mean-free-path l_s and the transport mean-free-path l_t . The scattering mean-free-path l_s is the length at which the intensity of a photon flux fallen onto the sample with no absorption is reduced by the factor $1/e$. It is also defined as the average distance between two scattering events. The transport mean-free-path l_t is defined as the average distance the light travels before its direction of propagation is randomized. In a weakly absorbing medium, the transport mean-free-path l_t is related to l_s by the expression

$$l_t = \frac{l_s}{1 - \langle \cos \theta \rangle}, \quad (1)$$

where $\langle \cos \theta \rangle = \bar{\mu}$ is the average cosine of the scattering angle (the asymmetric parameter). Depending on the application, the most adequate parameter describing scattering in the system can be l_t or l_s . Light propagation through a scattering medium or behavior of a random laser can best be described in terms of the transport mean-free-path l_t . At the same time, the scattering length l_s

may be a more useful parameter at evaluating the loss in a laser element placed in a regular laser cavity. The other characteristic parameter, which describes the photon propagation in scattering absorbing systems, is the inelastic mean-free-path l_i , which is the length of the light path along which intensity is reduced to $1/e$ of its initial value due to absorption.

Although there are several theoretical models to describe the light propagation in a scattering medium such as the Melamed model¹ or the Kubelka–Munk two flux model,² when the transport mean-free-path is much longer than the wavelength ($l_t \gg \lambda$), the propagation is commonly described by a photon diffusion model.^{3–5} The validity of the Melamed statistical approach is limited only to geometric optics approximation. On the other hand, the Kubelka–Munk model's main shortcoming is the complexity to relate the Kubelka–Munk constants to the intrinsic optical properties of the materials. In this work, we analyze the reflectance R and the transmittance T of a scattering slab in terms of the diffusion model, in which the effect of the anisotropy of scattering has been explicitly taken into account. In some works,^{3–5} the incoming light beam at the boundary is replaced by a source of diffuse radiation located at a certain plane inside the sample. The source of diffuse radiation considered in this paper is the propagating light beam, which intensity decays exponentially along the propagation path due to scattering and absorption. This source better approximates an experiment and allows for its accurate description and analysis.

Based on the developed theoretical model, we have designed and implemented the experimental technique to determine l_t and l_i in scattering samples. It is based on the measurements of transmission (in an integrating sphere setup) as a function of the sample thickness. We have applied the technique to translucent Nd:YAG ceramics synthesized in the Center for Materials Research at Norfolk State University and compared the results with the ones obtained using two known methods. In the first one, l_t was determined from the coherent backscattering (CBS) measurements.^{6–9} Another experiment was based on the on-axis transmission measurement conducted in a thin sample.

2. THEORETICAL MODELING OF TRANSMISSION AND REFLECTION

Let us consider a plane wave incident along the axis z upon a slab, whose dimensions x and y are much larger than the dimension z . The cross section of the light beam is also much larger than the dimension z . By assuming that the only source is light propagating along z , which decays exponentially as it propagates, $I_{\text{in}}(z) = J_0 \exp(-z/l^*)$, the steady-state diffusion equation describing the migration of photons can be written as²

$$\frac{\partial^2 U_d}{\partial z^2} - \frac{U_d}{l_{\text{abs}}^2} = -\frac{3J_0}{4\pi l_s} \left[\frac{1}{l_t} + \frac{\bar{\mu}}{l^*} \right] \exp\left(-\frac{z}{l^*}\right), \quad (2)$$

where $U_d(z)$ is the average diffuse intensity, $l_{\text{abs}} = \sqrt{l_t l_i/3}$ is the diffusive absorption length defined as the average distance between the beginning and the end points of paths of length l_i , and $l^* = [1/l_t + 1/l_s]^{-1}$ is the extinction mean-free-path. The diffuse flux vector $\vec{J}_d(z)$, defined by the power flow per unit area, is given by

$$\vec{J}_d(z) = \frac{J_0 l_t}{l_s} \bar{\mu} \exp\left(-\frac{z}{l^*}\right) \hat{z} - \frac{4\pi}{3} l_t \frac{\partial U_d}{\partial z} \hat{z}. \quad (3)$$

The boundary conditions have been determined on the assumption that the diffuse fluxes propagating from the boundaries inside the sample are due to the internal reflectivities at the sample surfaces. If internal reflectivities are introduced into the boundary conditions proposed by Ishimaru,² the latter can be rewritten for average intensities as

$$U_d(z=0) - \frac{2}{3} l_t h_0 \frac{\partial U_d}{\partial z}(z=0) + \frac{h_0 J_0 l_t \bar{\mu}}{2\pi l_s} = 0, \quad (4)$$

$$U_d(z=L) + \frac{2}{3} l_t h_L \frac{\partial U_d}{\partial z}(z=L) - \frac{h_L J_0 l_t \bar{\mu}}{2\pi l_s} \exp\left(-\frac{L}{l^*}\right) = 0, \quad (5)$$

where $h_0 = (1+r_0)/(1-r_0)$, $h_L = (1+r_L)/(1-r_L)$, r_0 and r_L are the internal average reflectivities at the sample surfaces ($z=0$ and $z=L$, respectively), and L is the thickness of the scattering sample. Note that the effect of the anisotropy of the scattering pattern has been taken into account both in the diffusion equation and the boundary conditions. The average internal reflectivity of the samples has been estimated from the Fresnel reflection coefficients $R(\theta)$ by means of the expression¹⁰

$$r = \frac{3R_2 + 2R_1}{3R_2 - 2R_1 + 2},$$

with

$$R_1 = \int_0^{\pi/2} R(\theta) \cos \theta \sin \theta d\theta, \quad R_2 = \int_0^{\pi/2} R(\theta) \times (\cos \theta)^2 \sin \theta d\theta. \quad (6)$$

The $R(\theta)$ coefficients have been calculated by taking as the effective refractive index of the random system, the Maxwell–Garnet effective refractive index.

The transmittance T of the slab is determined by the sum of the incoming flux $\vec{J}_{\text{in}}(z) = J_0 \exp(-z/l^*) \hat{z}$ and the diffuse flux $\vec{J}_d(z)$ [Eq. (3)] evaluated at the sample surface $z=L$ and normalized by the incident flux (J_0). At the same time, the diffuse reflectance R is due to the normalized diffuse flux evaluated at the sample surface $z=0$. By solving the diffusion equation [Eq. (2)] with the boundary conditions (4) and (5), the general expressions for the transmittance and the reflectance of the slab are expressed as

$$T = \frac{a + b \exp(-L/l^*) \cosh(L/l_{\text{abs}}) + c \exp(-L/l^*) \sinh(L/l_{\text{abs}})}{d \cosh(L/l_{\text{abs}}) + e \sinh(L/l_{\text{abs}})}, \quad (7)$$

$$R = \frac{f \exp(-L/l^*) + f \cosh(L/l_{\text{abs}}) + g \sinh(L/l_{\text{abs}})}{d \cosh(L/l_{\text{abs}}) + e \sinh(L/l_{\text{abs}})}, \quad (8)$$

where a, b, c, d, e, f , and g are the functions shown in the Appendix A, which depend on the internal average reflectivities at the sample surfaces, the asymmetry parameter, and the mean free paths. It has been assumed that the internal average reflectivities at the boundaries are identical, $r_0 = r_L = r$; so $h_0 = h_L = h = (1+r)/(1-r)$.

At large values of thickness ($L \gg l_{\text{abs}}$) and for media with weak absorption ($l_i, l_{\text{abs}} \gg l_s, l_t$), the general expressions for transmittance and reflectance are simplified to

$$T = \frac{2(2h+3)l_t}{4hl_t + 3l_{\text{abs}}} \exp\left(-\frac{L}{l_{\text{abs}}}\right), \quad (9)$$

$$R = \frac{3l_{\text{abs}} + (2h-3)l_t}{4hl_t + 3l_{\text{abs}}}. \quad (10)$$

Under these assumptions, the transmittance decays exponentially with the sample thickness L , whereas the reflectance is independent of L .

3. EXPERIMENTAL

The experimental samples were translucent pieces of Nd-doped YAG ceramics. Two samples (A and B) were produced following the technique schematically outlined in Ref. 11. The major steps of the process involved coprecipitation synthesis of Nd:YAG nanoparticles followed by the compaction and vacuum sintering of the ceramic. In the preparation of sample C, a mixture of Al_2O_3 , Y_2O_3 , and Nd_2O_3 nanopowders was compacted and then sintered. A combination of the uniaxial mechanical pressure (30 MPa)

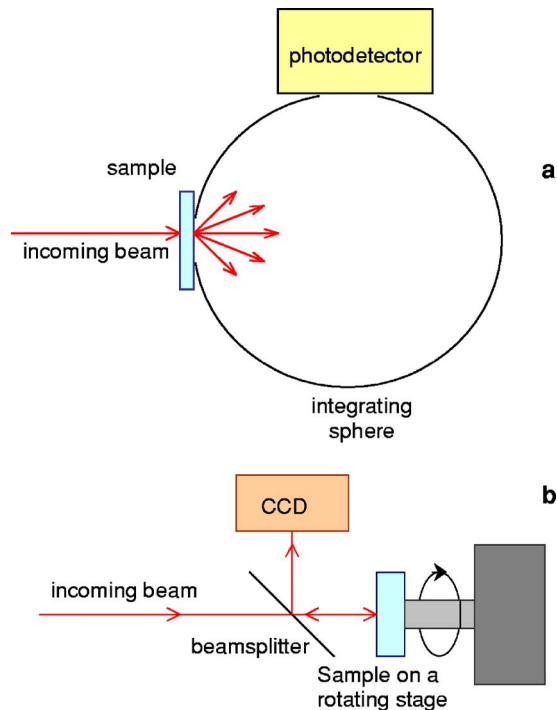


Fig. 1. (Color online) (a) Schematic of the transmission measurements in an integrating sphere, and (b) schematic of the CBS measurement.

and cold isostatic press (CIP, 450 MPa) was used in the preparation of pellets (~ 28 mm diameter). The maximal sintering temperature ranged between 1780 °C and 1800 °C. The sintered ceramics were characterized by the particle sizes d ranging between 5 and 10 μm . The relative density of the samples, normalized by the density of Czochralski grown 1% Nd:YAG (4.56 g/cm³) (Ref. 12) and evaluated with approximately 3% accuracy (relative variance measure), was equal to 96% for sample C, 89% for sample A, and 97% for sample B. Several plane-parallel polished plates, with the thickness ranging between ~ 0.15 and 1.6 mm, were prepared from each pellet. These samples were used in the transmission measurements as discussed below. In the coherent backscattering measurements, where the large sample thickness was important, we used stacks of plates.

Transmission measurements were conducted using the UV–VIS–IR spectrophotometer Lambda 900 from PerkinElmer. An integrating sphere was used in the measurements involving a series of samples of different thicknesses. The samples were attached to the front port of the integrating sphere [Fig. 1(a)]. On-axis transmission measurements in thin samples were done without an integrating sphere. CBS measurements were done in a standard setup. A CCD camera combined with a computer were used to record the CBS cone profiles [Fig. 1(b)].

4. RESULTS AND DISCUSSION

A series of transmission curves obtained in ceramic plates of different thicknesses is shown in Fig. 2. As follows from this figure, Nd absorption is practically absent in several spectral ranges. We chose such ranges for the evaluation of l_t since the applicability of Eq. (9) requires l_i, l_{abs}

$\gg l_s, l_t$. The dependence of the transmission (at $\lambda = 415$ nm) on the sample thickness measured in sample A is shown in Fig. 3. One can see that the dependence $T(L)$ becomes exponential at $L \geq 0.7$ mm. From the decay constant of the exponent, we determine $l_{\text{abs}} = 0.117$ cm, and from the intersection of the straight curve in Fig. 3 (exponential fit to the experimental data) and the vertical axis, we find $T_{\text{exp}}(0)$. Substituting l_{abs} , $T_{\text{exp}}(0)$, and $L = 0$ into Eq. (9), we arrive at $l_t = 0.014$ cm. In this calculation, we used $h = 5.23$ corresponding to the internal reflectivity r equal to 67.8%. The value of the internal reflectivity has been estimated from the Fresnel reflection coefficients¹⁰ by taking the effective refractive index of the scattering system given by the Maxwell–Garnet theory ($n \cong 1.70$ for a relative density of 89% corresponding to sample A).

Knowing l_{abs} and l_t , one can calculate (from $l_{\text{abs}} = \sqrt{l_t l_i}/3$) the value of the inelastic scattering length $l_i = 2.9$ cm. The corresponding absorption can be due to color centers or unwanted contamination of the material. Thus, the developed technique allows for one to evaluate both characteristic lengths in scattering samples, l_t and l_i .

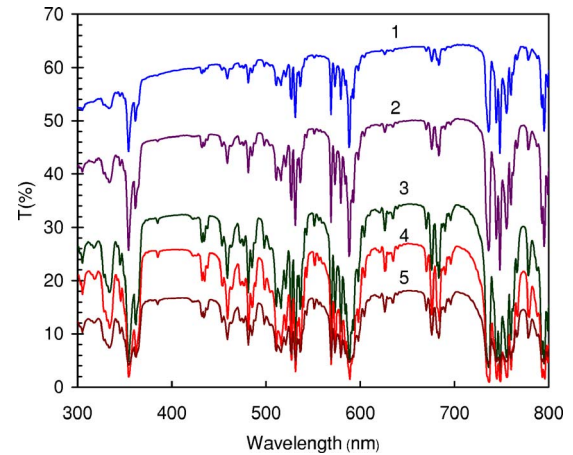


Fig. 2. (Color online) Transmission spectra of plates with different thicknesses (sample A). 1, 0.015 cm; 2, 0.028 cm; 3, 0.071 cm; 4, 0.094 cm; and 5, 0.147 cm.

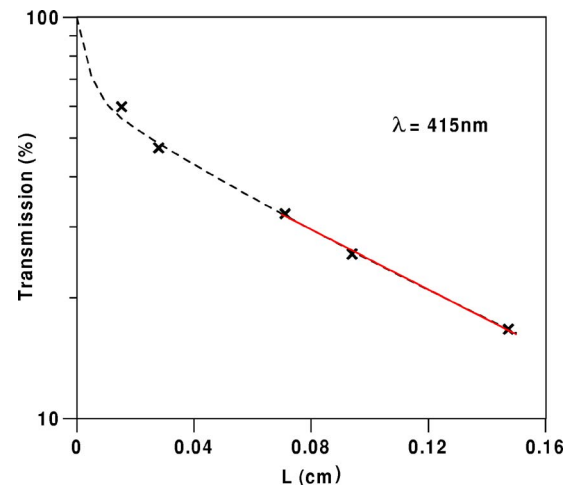


Fig. 3. (Color online) Transmission measured at 415 nm as a function of the plate thickness (sample A). The solid curve is the exponential fit ($L \geq 0.7$ mm), and the dashed curve is the curve obtained from the general expression for transmittance, Eq. (7).

The characteristic scattering and absorption lengths determined at $\lambda=415, 548, 650,$ and 841 nm, the wavelengths at which the Nd absorption is practically nonexistent, are summarized in Table 1. One can see that the values l_t measured in low-absorbing spectral regions are in good agreement with each other and are practically independent of the light wavelength. This behavior can be due to the weak wavelength dependence of light scattering when particle size is much larger than the wavelength. At these wavelengths, $l_i, l_{\text{abs}} \gg l_t$, which corresponds to the range of applicability of Eq. (9). The experimental error in the determination of l_t and l_i was $\pm 10\%$.

The same table shows the absorption coefficients of the Nd:YAG crystal¹³ at a Nd concentration equal to 2%. At the wavelengths where the sample absorption is significantly high (730, 731, and 732 nm), Eq. (9) fails. An increase of the absorption coefficient (k_{abs}) implies a shortening of l_i and consequently a reduction of l_{abs} . It can be seen in Table 1 that the experimentally measured values l_{abs} at 730, 731, and 732 nm are shorter than the values l_{abs} measured at the other wavelengths where the absorption is lower. However, the inelastic mean free paths at 730, 731, and 732 nm wavelengths obtained through Eq. (9) show just the opposite behavior, that is, they are higher. This is the reason why we can say that Eq. (9) fails where the absorption is appreciably high and the transport mean free paths obtained from Eq. (9) corresponding to 730, 731, and 732 nm wavelengths are not correct. Note that this experimental technique was relevant to the one proposed in Ref. 14, where the series of transmission measurements was done in a wedge-shaped sample.

The angular distribution of the scattered light intensity recorded at $\lambda=514.5$ nm in the CBS experiment in a stack of plates with the total thickness equal to ~ 3 mm is shown in Fig. 4. As shown in Ref. 15, in powders of Nd-doped materials at $k_{\text{abs}}l_t < 10^{-2}$, the value l_t calculated using the simple formula

$$l_t \approx 0.7 \frac{\lambda}{2\pi W}, \quad (11)$$

where W is the full width of the CBS cone at its half maximum, is almost the same as that obtained from a more accurate curve fitting taking absorption into account. Applying Eq. (11) to our experimental data, we have determined l_t to be equal to 0.019 cm. Note that the signal in the CBS experiment was weak and noisy. Thus, the

measured value l_t had a relatively large experimental error ($\pm 20\%$).

The third experimental technique we used was based on on-axis transmission measurements in thin samples. If a collimated light beam of intensity I_{in} is falling onto a slab of thickness L , the intensity of output light I_{out} measured on axis in a small solid angle is given by

$$I_{\text{out}} = I_{\text{in}} \exp(-L/l^*) = I_{\text{in}} \exp(-L(1/l_s + 1/l_i)). \quad (12)$$

Assuming that at $\lambda=415$ nm, $l_i \gg l_s$ and using Eq. (12), we determined experimentally in sample A, $l_s=0.0031$ cm. Taking an effective particle size of $7.5 \mu\text{m}$ and assuming the spherical shape of a particle, Mie theory yields for the average cosine of the scattering angle $\langle \cos \theta \rangle = 0.733$. Hence, according to Eq. (1), l_t should be equal to 0.0116 cm, which is in fairly good agreement with the values obtained in the previous methods for sample A (see Table 2). Anyway, this last value cannot be expected to give a more accurate estimation of l_t since the size distribution of the particles is broad and their shape is not spherical. Moreover, the high concentration f of particles implies that correlations among the scatterers should be taken into account and other more appropriate theories should be applied in order to correctly explain the transport properties of these high dense random materials.¹⁶

The values of the transport mean-free-path l_t (based on the measurements conducted in a series of slabs of different thicknesses) were determined in samples B and C. The results of the measurements are presented in Table 2 along with the photographs of ≈ 0.3 mm thick plates of the three samples studied. One can see an unambiguous

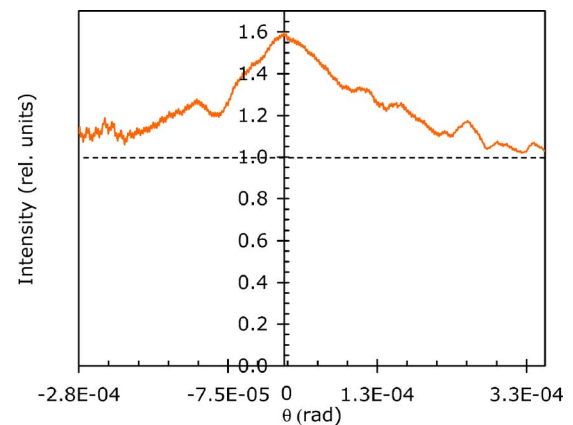

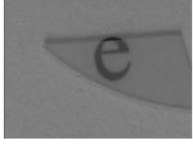



Fig. 4. (Color online) CBS profile measured in sample A at $\lambda=514.5$ nm.

Table 1. Characteristic Scattering and Absorption Lengths Determined in Sample A Based on the Results of the Transmission Measurements

λ (nm)	415	548	650	841	730	731	732
k_{abs} (cm^{-1}) in grown Nd:YAG	~ 0	~ 0	~ 0	~ 0	2.5	1.8	1.2
l_{abs} (cm)	1.17×10^{-1}	1.15×10^{-1}	1.21×10^{-1}	1.18×10^{-1}	9.94×10^{-2}	9.85×10^{-2}	9.83×10^{-2}
l_t (cm)	1.4×10^{-2}	1.4×10^{-2}	1.5×10^{-2}	1.4×10^{-2}	0.85×10^{-2}	0.71×10^{-2}	0.52×10^{-2}
l_i (cm)	2.9	2.8	2.9	2.9	3.5	4.0	5.6
determined from l_{abs} and l_t							

Table 2. Transport Mean-Free-Paths in Three Samples Studies Measured by Different Techniques

Sample	A	B	C
Photographs of ~0.3 mm polished samples			
Transmission in a series of thick samples (415 nm)	1.4×10^{-2} cm	3.9×10^{-2} cm	0.86×10^{-2} cm
Coherent backscattering (514.5 nm)	1.9×10^{-2} cm		
On-axis transmission in thin samples (415 nm)	1.16×10^{-2} cm		

correlation between the measured value of the transport mean free path and the transparency of the sample. This is another confirmation of the adequacy of the measurement. (Note that samples A, B, and C are not among the most transparent YAG ceramic samples developed in the Center for Materials Research at Norfolk State University).¹⁷

5. SUMMARY

We have obtained expressions describing reflection and transmission of scattering samples in diffusion approximation for random media with weak absorption and large thickness. In this model, the source is the extinguished light of the incoming beam which decays exponentially along its propagation in the scattering sample. Based on the transmittance expression, we have designed and implemented an experimental technique to determine the transport mean free path and the inelastic mean free path in scattering materials. The adequacy of the developed method has been proven by comparison of the experimental results with the ones obtained using the CBS technique and on-axis transmission measurements. Besides, a clear correlation between the experimentally determined values of the transport mean free path and the visible translucence of the samples has been observed.

APPENDIX A: EXPRESSIONS FOR FUNCTIONS

The expressions for the functions a , b , c , d , e , f , and g corresponding to Eqs. (7) and (8) are

$$a = l_i^2 \frac{l_t}{l_{\text{abs}}} [3l_i l_s + (3\bar{\mu}(l_i + l_s) + 2h(l_i + 3\bar{\mu}l_s + l_s))l_t], \quad (\text{A1})$$

$$b = l_i \frac{l_t}{l_{\text{abs}}} [-3l_i l_s (l_i + 4hl_s) + (-3\bar{\mu}l_i(l_i + l_s) + 2h(l_i^2 - 3(\bar{\mu} - 1)l_i l_s + 2l_s^2))l_t], \quad (\text{A2})$$

$$c = (-9l_i^2 l_s^2 - 3l_i l_s (2h + 3\bar{\mu} - 1)l_i + (4h^2 - 1)l_s)l_t + 2h(l_i + l_s)(2h(l_i + l_s) - 3\bar{\mu}l_i^2), \quad (\text{A3})$$

$$d = 12hl_{\text{abs}}((l_i + l_s)^2 l_t - 3l_i l_s^2), \quad (\text{A4})$$

$$e = ((l_i + l_s)^2 l_t - 3l_i l_s^2)(4lh^2 + 3l_i), \quad (\text{A5})$$

$$f = 3l_{\text{abs}}[l_i(-3l_i l_s + (-3\bar{\mu}(l_i + l_s) + 2h(l_i + 3\bar{\mu}l_s + l_s))l_t)], \quad (\text{A6})$$

$$g = 9l_{\text{abs}}^2[l_i(l_i - 2hl_s + 3\bar{\mu}l_s + l_s) - 2h\bar{\mu}l_i(l_i + l_s)]. \quad (\text{A7})$$

ACKNOWLEDGMENT

This work was supported by the NASA grant NCC-3-1035, the National Science Foundation (NSF) grant HRD-0317722, and the NSF grant PREM DMR-0611430. This work was also supported by the Spanish Government Ministerio de Educación y Ciencia (MAT2004-03780) and the Basque Country University (UPV13525/2001). The

authors acknowledge the help of Ren-Guan Duan, Ichesia Veal, Kevin Reynolds, Yuri Barnakov, and Guohua Zhu for providing the experimental samples and assistance with their characterization.

M. A. Illarramendi's e-mail address is mariaasuncion.illarramendi@ehu.es.

REFERENCES AND NOTES

1. N. T. Melamed, "Optical absorption coefficients and the absolute value of the diffuse reflectance," *J. Appl. Phys.* **34**, 560–570 (1963).
2. A. Ishimaru, *Wave Propagation and Scattering in Random Media* (IEEE, and Oxford U. Press, 1997).
3. A. Z. Genack and J. M. Drake, "Relationship between optical intensity, fluctuations and pulse propagation in random media," *Electron. Lett.* **11**, 331–336 (1990).
4. N. Garcia, A. Z. Genack, and A. Lisyansky, "Measurement of the transport mean path of diffusing photons," *Phys. Rev. B* **46**, 14475–14479 (1992).
5. J. Gomez-Rivas, R. Sprik, A. Lagendijk, L. D. Noordam, and C. W. Rella, "Static and dynamic transport of light close to the Anderson localization transition," *Phys. Rev. E* **63**, 046613 (2001).
6. M. P. van Albada and A. Lagendijk, "Observation of weak localization of light in random medium," *Phys. Rev. Lett.* **55**, 2693–2695 (1985).
7. P. E. Wolf and G. Maret, "Weak localization and coherent backscattering of photons in disordered media," *Phys. Rev. Lett.* **55**, 2696–2699 (1985).
8. P. E. Wolf, G. Maret, E. Akkermans, and R. Maynard, "Optical coherent backscattering by random media: an experimental study," *J. Phys. (France)* **49**, 63–75 (1988).
9. M. B. van der Mark, M. P. van Albada, and A. Lagendijk, "Light scattering in strongly scattering media: multiple scattering and weak localization," *Phys. Rev. B* **37**, 3575–3592 (1988).
10. J. X. Zhu, D. J. Pine, and D. A. Weitz, "Internal reflection of diffusive light in random media," *Phys. Rev. A* **44**, 3948–3959 (1991).
11. J. Lu, K. Ueda, H. Yagi, T. Yanagitani, Y. Akiyama, and A. Kaminski, "Neodymium doped yttrium aluminum garnet ($\text{Y}_3\text{Al}_5\text{O}_{12}$) nanocrystalline ceramics—a new generation of solid state laser and optical materials," *J. Alloys Compd.* **341**, 220–225 (2002).
12. W. Koechner, *Solid-State Laser Engineering*, 5th ed. (Springer-Verlag, 1999).
13. The reference absorption spectrum of a 1% Nd-doped Czochralski-grown YAG crystal was done by Michael Bass, College of Optics and Photonics, University of Central Florida.
14. A. Z. Genack, "Optical transmission in disordered media," *Phys. Rev. Lett.* **58**, 2043–2046 (1987).
15. M. Bahoura and M. A. Noginov, "Determination of the transport mean free path in a solid-state random laser," *J. Opt. Soc. Am. B* **20**, 2389–2394 (2003).
16. K. Busch, C. M. Soukoulis, and E. N. Economou, "Transport and scattering mean free paths of classical waves," *Phys. Rev. B* **50**, 93–98 (1994).
17. Yu. A. Barnakov, I. Veal, Z. Kabato, G. Zhu, M. Bahoura, and M. A. Noginov, "Simple route to Nd:YAG transparent ceramics," in *Laser Source and System Technology for Defense and Security II*, G. L. Wood and M. A. Dubinskii, eds., Proc. SPIE **6216**, 62160Z (2006).